CORRUGATION MODELS AND THE ROARING RAILS ENIGMA:
A SIMPLE ANALYTICAL CONTACT MECHANICS MODEL
BASED ON A PERTURBATION OF CARTER'S SOLUTION

Luciano Afferrante and Michele Ciavarella

CORRUGATION MODELS AND THE ROARING RAILS ENIGMA:
A SIMPLE ANALYTICAL CONTACT MECHANICS MODEL
BASED ON A PERTURBATION OF CARTER'S SOLUTION

LUCIANO AFFERRANTE AND MICHELE CIAVARELLA

Corrugation in railways, and especially short pitch corrugation (30–80 mm), is still considered something of an enigma, despite extensive research. Models based on repeated impacts or differential wear, such as Grassie and Johnson's (1985) and Bhaskar et al.'s (1997), seem not to be conclusive, or not to suggest the correct wavelength.

Further models have been suggested, either linear (Frederick, Valdivia, Hempelmann, Vassily and Vincent) or nonlinear (Mueller), but most suggest a constant frequency mechanism invariably connected to vertical resonances of the system either in the low frequency range (50–100 Hz, the resonance of the vehicle's unsprung mass on the track stiffness referred to here as the "P2 resonance", close to the Hertz contact resonance), or at about 1000 Hz (pinned-pinned resonance, in which the rail vibrates almost as if it were a beam pinned at sleepers), or even higher frequencies still (1700–1800 Hz). The experimental data available, by contrast, do not fit these frequency ranges. The discrepancy is tentatively explained with "contact filtering" and varied traffic ideas, but do not convince completely.

In this paper, we stress the importance of wheel inertia in coupling the oscillations of normal load, with the variations of tangential load and longitudinal creepage. A simple zeroth order perturbation of the classical rolling contact solutions is suggested, which obtains good qualitative agreement with experimental evidence. The model also leads to the recognition that vertical resonances are not crucial in explaining corrugation, as believed in previous models, since we use an extremely simple model of an Euler beam with no elastic support, having no resonances. Important factors for the growth of corrugation are the friction coefficient and the tractive ratio. High longitudinal creepage is needed to promote rapid development, and this can arise from curving, hunting motion or misaligned axles, and is probably exacerbated by high contact conformity, since this increases the fluctuating component of longitudinal creepage due to the movement of the contact point. With discrete supports, we expect a modulation of corrugation wavelength and amplitude, but this requires a separate investigation, not just the inclusion of pinned-pinned resonance.

1. Introduction

Corrugations have been observed and studied for more than a century, and many tentative explanations have been put forward, but none seems convincing for short-pitch rail corrugation ("roaring rails") in the range of 20–80 mm wavelength [Grassie and Kalousek 1993]. This is because a nonproportional increase in corrugation wavelength with increasing trains speed is observed, as in Figure 1 of [Bhaskar et al. 1997a], which displays data from a 1911 BR report, David Harrison's thesis data (1979), and the Vancouver SkyTrain metro system data.

This makes simple vertical resonance models unsuccessful, and calls for nonlinear effects, or a threshold. For example, a simple mass vertically suspended on a spring-and-damper system — a model used to attempt to explain corrugation of roads, a process known in North America as washboarding (see [Both et al. 2001] and references therein, the more recent [Hoffmann and Misol 2007], and also http://en.wikipedia.org/wiki/Washboarding and its external links) predict that instability occurs for all wavelengths larger than a critical value linearly dependent on speed, which depends on the properties of the vehicles and the road surface. However, the wavelength observed in roads seems typically to correspond to frequencies one or two orders of magnitude higher than the lowest vertical resonance of the system.

Similar troubles emerge when attempting to use such simple models for railway corrugation, since the Hertz spring contact resonance model suggested by Carson and Johnson [1971], and observed in twin-disk machines in [Johnson and Gray 1975], suggests a frequency which is highly damped, and hence the normal impact mechanism inducing plastic deformations is observed only at higher wavelengths. Frederick [1987], from BR research, reports that plastic deformation occurs on the peaks where at the short-pitch corrugation frequency corresponds indeed the peak of the normal force, but not on the troughs. There is a need to an alternative explanation for short pitch corrugation, perhaps competing with the plastic deformation mechanism. Indeed, Frederick also reports that high plastic deformation resistant material show corrugation quickly, although the increase of wear resistance slows the rate of formation. Other general observations were given in the well known paper [Grassie and Kalousek 1993], namely that short pitch corrugation is (i) primarily observed on high-speed track, at 100–250 km/h; (ii) mainly on tangent track and on large radius curves with relatively low axle loads; and (iii) with wheel-rail excitation in the frequency range 350–2800 Hz. The first two observations clearly point at a phenomenon which requires sufficient energy to develop and probably sufficient creepage.

A model based on differential wear was then proposed by Grassie and Johnson [1985]. They calculated the frictional energy dissipation in the slip zone of the contact patch as a wheel rolls over a sinusoidally corrugated rail. However, since they assumed a *constant longitudinal creepage* (perhaps under the assumption that the large mass of the vehicle would stop the rotational speed of the wheel to change?), the phase of wear remained very close to the peak of normal force (close to the crests), promoting a mechanism for reduction of corrugation in the frequency range of interest. There was no maximum in the energy dissipation at a particular fixed wavelength independent of vehicle speed, and at typical speeds, the predicted phase did not correspond to a wear maximum in the troughs of an existing corrugation.

This attempt certainly became well known in railways industries and other academic contexts where corrugation was heavily studied, mainly BR, Berlin University, and later Chalmers in Sweden. Assuming that Grassie and Johnson showed longitudinal creepage removed corrugation, the possibility of traction or braking was not included in some later models, and a fortiori the inertia of the wheel and the rotational dynamics of the system were neglected. We can gather this impression from Frederick, head of research at BR, who in a discussion to the paper [Hempelmann and Knothe 1996] asks why not including longitudinal creepage, since it is known to be generally larger than lateral creepage, "although likely to suppress corrugation".

Frederick [1987] first suggested a perturbation analysis of the nonlinear relationships between normal and tangential forces, creepage and wear, and using complex functions transfer functions, valid for both longitudinal as well as lateral creepage, for defining conditions for which the phase of dissipation would

be such that the component out-of-phase with the initial wave could progress. Unfortunately, many details of the models are very crudely represented. The corrugation is found to be enhanced if there is in the initial rail energy in the frequency range 800–900 Hz which correspond to surface profile positioned near or over a sleeper, attributed to a high vertical impedance and low lateral impedance of the rail. Frederick suggests that it may be possible that extending the analysis to lower frequencies, another high impedance may be found when the sleepers vibrate in antiphase to the rail. The results are however probably affected by the many assumptions in the model.

To explain the discrepancies, Frederick [1987] and Valdivia [1988b; 1988a] have introduced the idea of a "contact filter" , so that in fact the dynamic contact force is mostly amplified in a narrow band of frequency. In particular, for lower speed traffic, the filter makes the pin-pin frequency band "inactive" because it would produce corrugation at less than 1.5 times the contact patch length (i.e. about 20 mm). The 300–400 Hz band is then active (P2 resonance), but that, again, roughly produces corrugations of the observed wavelength. Mixed traffic can reinforce waves of roughly the same pitch. However, this idea of "contact filter" was never really validated.

Significant progress was made by the group of Prof. Knothe in Berlin, and at the Charmec research centre of Chalmers University in Sweden. Groß-Thebing [1993] looked at the transient dynamics effect devising a numerical method using the program CONTACT by Kalker defining generalized complex Carter coefficients to define the tangential load harmonic oscillations due to perturbation of the steady state for harmonic creepage. This code was used in [Hempelmann and Knothe 1996; Hempelmann 1994] but unfortunately, concentrating on lateral creepage alone. Hempelmann also attempts to take into account the discrete nature of support of the rail, although with a spurious Fourier analysis not allowing for parametric resonance; in [Hempelmann and Knothe 1996], the authors attributes the corrugation wavelength to pinned-pinned resonance at about 1000 Hz. This resonant frequency (or more precisely, the slightly higher antiresonance) may indeed have some effect in corrugation, but Hempelmann's results do not seem to show this, whereas Müller [1998] in his more sophisticated nonlinear version, seems to conclude corrugation to correspond to the low vertical receptance at approximately 1000 Hz, although he also shows that other structural dynamics effects can also dominate the profile development, e.g. the high lateral rail receptance between 1600 and 1800 Hz and the low vertical rail receptance near 300 Hz.

Bhaskar et al. [1997a; 1997b] looked at the Vancouver SkyTrain tramway system where no traction or braking is done at the wheels, yet longitudinal creepage "can arise from curving, hunting motion or misaligned axles", and indeed their reference case has three comparable components of steady creepage. However, the fluctuating parts of creepage are only caused by conformity ("principal cause of fluctuating longitudinal creepage was found to be the fluctuation in rolling radius due to the movement of the contact point [see equation (27) in [Bhaskar et al. 1997a], which is almost in phase with the angular ripple at most frequencies"), whereas rotational inertia of the wheelset is not included in the model, nor its complete receptance. Incidentally, these authors also attempted to simplify the results of the Groß-Thebing method fitting some results with a spring and dashpot in series at the contact: in particular, the stiffness of the spring is estimated by from a static Mindlin problem, and the dashpot from the zero-th order perturbation of the Carter-like steady state rolling contact solution. However, all this is based on a single fitting of Groß-Thebing's results with oscillating longitudinal creepage and constant normal load, so while it is likely that the method has sufficient validation for pure oscillation of tangential load alone, the authors do not indicate how to estimate energy dissipation in the general case, and indeed only use the damping term

(no transient effects) in most later calculations — as it will be done in the present paper, which therefore is the equivalent of their paper with no account of conformity of the contact, but with the addition of inertia of the wheel and its dynamics.

It is surprising that the corrugation literature is vast and spans more than a century (Sato et al. [2002] estimate about 1500 papers), yet true comparisons between models and a careful consideration of the critical ingredients have not been attempted in the literature, leaving the impression that only extremely sophisticated models (and accordingly, accurate measurements for many parameters) could reproduce the phenomenon. We shall return to this later, when our simple model will indeed be developed in this paper.

Towards a simple model. A recent paper [Grassie and Edwards 2008] attracted our attention and motivated the present study. The first author is clearly one of the leading authorities in the field of corrugation, being one of the authors of the influential paper [Grassie and Johnson 1985] two decades ago, which however was unsuccessful in that the corrugation phase could not correspond to the trough of the profile. Hence, it was natural to compare the approaches of the two papers to see what was wrong in the early paper. [Grassie and Edwards 2008] distinguishes between corrugation initiated (i) as a result of a varying normal load with essentially constant tangential load — applied traction and braking, steering forces or a combination of the two — (ii) from a varying tangential traction with essentially constant normal load, and (iii) occasionally as a result of a combination of the two. Case (i) is said to be associated to either the resonance of the vehicle's unsprung mass on the track stiffness referred to here as the "P2 resonance" (typically in the range 50–100 Hz) or the "pinned-pinned resonance" of the rail (typically at much higher frequencies, around 1000 Hz), in which this vibrates almost as if it were a beam pinned at sleepers. This second resonance is called the "dominant wavelength-fixing mechanism for main-line corrugation". This association did not appear very rigorous, but one immediate reaction on this classification was that the normal load would vary as a result of corrugation or roughness on the railway, and hence its oscillation would indeed be in the range of high frequency. Therefore, it would be difficult to assume that tangential load could be constant also in this frequency unless the inertia of the wheel were very low, giving the first ingredient added in the present paper. However, the extremely simple analytical estimate of differential wear from the energy dissipation in the steady state fluctuating only as a result of the fluctuations of creepage from varying normal load, seem to qualitatively fit some experimental data. This results into a brutally simple equation, but no check is made on the *phase* of the differential energy dissipation, which had been the trouble in the earlier [Grassie and Johnson 1985]. Trusting Grassie's intuition had pointed in the correct direction, we were therefore motivated to investigate more.

We shall try to consider if it is possible to include only just enough ingredient to explain corrugation, more precisely checking the issues raised by Grassie and Edward within a simple, analytical, perturbation of a Carter solution, in the form including 3D effects in Bhaskar et al. Removing the hopes to include transient effects with the spring+dashpot model, because we believe that the transient effects would anyway require separate and sophisticated treatments, we permit nevertheless both tangential load and creepage to oscillate. Then, we shall consider the phase of the differential energy dissipation, to see if the negative conclusions of Grassie and Johnson apply also to this more general case.
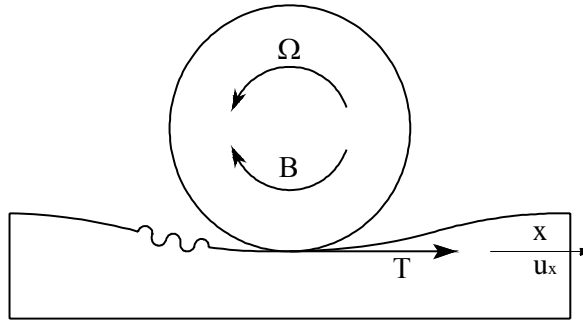
Figure 1. The model under investigation.

2. The model

We shall consider a 2D model with vertical and rotational degrees of freedom (Figure 1). The rail is corrugated in the simple form

$$\Delta \exp(\iota \omega t),$$

where $\omega = 2\pi V/\lambda$; here V is the velocity of the train and λ the corrugation wavelength. Finally, Δ is the amplitude of corrugation, which is up to about $100\,\mu$m when full unloading occurs and a linear model is no longer possible, although the noise would become so large that this is prevented in most maintenance strategies. We suppose the normal problem is independent of the tangential problem and results in a normal force

$$P = P_0 + P_1 \exp(\iota \omega t). \tag{1}$$

We linearize about a given steady state, given by the mean value normal force P_0, tangential force Q_0, and creep ratio ξ_0. We will linearize the contact stiffness in the vertical and tangential direction, and make a perturbation of the steady state solution, to estimate the tangential velocities in the contact area.

The *steady state* creep ratio ξ_0 is defined as the relative velocity of the rail with respect to the wheel

$$\xi_0 = 1 - \frac{\Omega_0 R}{V} = \frac{\partial u_0}{\partial x}, \tag{2}$$

where we are assuming braking conditions, so $\Omega_0 R < V$ and $\xi_0 > 0$.

In the transient conditions, the local sliding velocity is a function of both x and t. We can define the transient creepage as the instantaneous rigid body velocity of the rail (V) and that of the wheel ($\Omega(t)R$) — i.e. the rigid body creepage

$$\xi(t) = 1 - \frac{\Omega(t)R}{V}, \tag{3}$$

The perturbative approach will work well if things don't change too fast relative to the motion of the contact region. In a solution with only longitudinal creepage, perturb (3) about Ω_0, ξ_0, to have

$$\xi - \xi_0 = -\frac{(\Omega - \Omega_0)R}{V} \tag{4}$$

We introduce a 3D solution equivalent to Carter's; it is also described in [Bhaskar et al. 1997a, (5a)], as the longitudinal creep ratio (we assume no lateral creep)

$$\xi = \xi_{\max} \left[1 - \left(1 - \frac{Q}{\mu P} \right)^{1/3} \right], \tag{5}$$

where Q is the resulting tangential force which is only in the x-direction, and $\xi_{\max}$ is given by[1]

$$\xi_{\max} = \frac{3\mu}{C_{00}} \left[\frac{16P}{9(1-\nu)^2 R_e^2 G} \right]^{1/3}, \tag{6}$$

with the Kalker's creep coefficient expressed approximately as a function of a/b

$$C_{00} = 2.84 + 1.2\frac{a}{b} \approx 2.84 + 1.2 \left(\frac{R_1}{R_2} \right)^{2/3}, \tag{7}$$

so that (5) can be rewritten as

$$Q = \mu P \left(1 - \frac{(\xi_{\max} - \xi)^3}{\xi_{\max}^3} \right).$$

It then follows that the dissipation in the steady state is

$$W_0 = V\xi_0 Q_0 = \mu P_0 V \left(1 - \frac{\Omega_0 R}{V} \right) \left(1 - \frac{(\xi_{\max} - 1 + \Omega R/V)^3}{\xi_{\max}^3} \right), \tag{8}$$

where we have substitute for ξ the expression $\xi = 1 - \Omega R/V$ and $\xi_{\max}$ is a function of P, according to (6). Hence, by differentiation, we obtain the zero-th order perturbation as

$$Q_P = \frac{\partial Q}{\partial P} \bigg|_{P_0,\Omega_0} = \frac{2\mu\xi_0}{\xi_{\max}} \left(1 - \frac{\xi_0}{2\xi_{\max}} \right); \tag{9}$$

$$Q_\Omega = \frac{\partial Q}{\partial \Omega} \bigg|_{P_0,\Omega_0} = -\frac{3\mu R P_0}{V\xi_{\max}} \left(1 - \frac{\xi_0}{\xi_{\max}} \right)^2; \tag{10}$$

$$W_P = \frac{\partial W}{\partial P} \bigg|_{P_0,\Omega_0} = \frac{2\mu V\xi_0^2}{\xi_{\max}} \left(1 - \frac{\xi_0}{2\xi_{\max}} \right) = V\xi_0 Q_P; \tag{11}$$

$$W_\Omega = \frac{\partial W}{\partial \Omega} \bigg|_{P_0,\Omega_0} = -\frac{6\mu P_0 R\xi_0}{\xi_{\max}} \left[1 - \frac{3\xi_0}{2\xi_{\max}} \left(1 - \frac{4\xi_0}{9\xi_{\max}} \right) \right]. \tag{12}$$

The fluctuating parts of tangential load and dissipation can therefore be written in the form

$$Q_1 = Q_P P_1 + Q_\Omega \Omega_1 \tag{13}$$

$$W_1 = W_P P_1 + W_\Omega \Omega_1. \tag{14}$$

---

[1]We are defining the Kalker coefficients as positive, for simplicity, and hence change the sign of the creep-load relationships as more commonly found in the literature.

Coupling with the dynamics. The dynamic equilibrium of the wheelset, which we simplify now with no stiffness or damping, gives

$$I_w \frac{d\Omega}{dt} = (Q - Q_0)\, R \tag{15}$$

where I_w is the inertia of the wheel. Moving to the oscillatory parts therefore, (15) reduces to

$$\iota\omega I_w \Omega_1 = Q_1 R \tag{16}$$

Substituting Ω_1 from (16) into (13), we have

$$Q_1 = Q_P P_1 + Q_\Omega \frac{Q_1 R}{\iota\omega I_w}, \tag{17}$$

and collecting Q_1, we can write the tangential load oscillatory term in the perturbation as a function of the oscillatory term in normal load only,

$$Q_1 = \frac{Q_P}{1 - Q_\Omega R/(\iota\omega I_w)} P_1. \tag{18}$$

For dissipation, substituting Ω_1 from (16) into (14), we have

$$W_1 = W_1 = W_P P_1 + W_\Omega \frac{R}{\iota\omega I_w} Q_1 = Q_P \left(V\xi_0 + \frac{W_\Omega}{\iota\omega I_w/R - Q_\Omega} \right) P_1 \tag{19}$$

In dimensionless form we can define the dissipated power $\hat{W}_1 = W_1/(\mu P_0 V\xi_0)$ as

$$\hat{W}_1 = \frac{2\xi_0}{\xi_{\max}} \left(1 - \frac{\xi_0}{2\xi_{\max}} \right) \left(1 - \frac{6}{\xi_{\max}} \cdot \frac{1 - \frac{3\xi_0}{2\xi_{\max}} \left(1 - \frac{4\xi_0}{9\xi_{\max}} \right)}{\iota\hat{I}_w\zeta + \frac{3}{\xi_{\max}} \left(1 - \frac{\xi_0}{\xi_{\max}} \right)^2} \right) \frac{P_1}{P_0} \tag{20}$$

where we have introduced the following dimensionless terms

$$\hat{I}_w = \frac{I_w V^2}{2\mu P_0 a_0 R^2}; \qquad \zeta = \frac{2\omega a_0}{V} = \frac{4\pi a_0}{\lambda}. \tag{21}$$

where a_0 is the semiwidth of contact in longitudinal direction

$$a_0 = \left(\frac{3\,(1 - \nu)\, R R_e P_0}{4 G R_r} \right)^{1/3} \tag{22}$$

and $R_e = \sqrt{R R_r}$ with R the rolling radius of the wheel and R_r the other relative radius of curvature between the wheel and the rail.

Because microslip and dissipation for a small imposed creep occur towards the rear of the contact, whereas the present calculation associates dissipation with the position of the wheel, the lag of dissipation at a point on the rail is overestimated by about $2\pi a_0/\lambda = \zeta/2$. For this reason the phase of W_1 is corrected by introducing a phase lag of $-2\pi a_0/\lambda$. However when the tractive ratio is large, near to full sliding conditions, dissipation occur nearer the centre of the contact area. In this case the lag of dissipation at a point on the rail is overestimated by about $\pi a_0/\lambda = \zeta/4$. In between full stick, and full slip, we assume a linear variation of this correction.

Vertical dynamic model. When the frequency of interest for corrugation is greater than about 500 Hz, the dynamics is dominated by that of the rail described with a simple Euler beam model, not even requiring the inclusion of the elastic supports usually described with Winkler foundations: an infinite beam subjected to a stationary force and whose magnitude oscillates in time at frequency $f = \omega/2\pi$. The mathematical description of the beam model is obtained from the case of load moving with speed V given in the Appendix, although it has certainly been obtained elsewhere previously. For validation and comparison, we shall use the more sophisticated model of Bhaskar et al. [1997a; 1997b], where the rail is continuously supported by uniformly distributed rail pads, sleeper mass and ballast. The effect of discrete sleepers in that work was neglected, because the SkyTrain system has mostly a continuous support.

3. The model

Figure 2 shows the variation with the frequency of the amplitude and phase of the vertical receptance. With solid line we plot the receptance of an infinite beam subjected to a force that moves at speed V, with dashed line the receptance of the model of rail presented in [Bhaskar et al. 1997a]. The comparison is done for $m_{\text{rail}} = 56$ kg/m, $V = 27.8$ m/s and $I_{\text{rail}} = 2.35 \times 10^{-5}$ m^4 as typical values.

For their model, a sharp resonance peak is found at about 100 Hz, corresponding to a vibration mode in which the loaded track vibrates as a whole on the flexibility of the ballast. However, this mode of vibration has been associated with the long wavelength corrugations (greater than 200 mm), which display severe plastic deformation in their troughs. Short pitch corrugation is associated with much higher frequencies (corresponding to wavelength in the range of 20–80 mm), and for high frequencies we note the similarity between the Bhaskar model and the present beam model in terms of the asymptotic value of vertical receptance, for which we get (see Appendix)

$$H_{\text{rail}} = \frac{\exp(-\iota 3\pi/4)}{2\sqrt{2}\left(m_{\text{rail}}^3 E I_{\text{rail}}\right)^{1/4} \omega^{3/2}}. \tag{23}$$
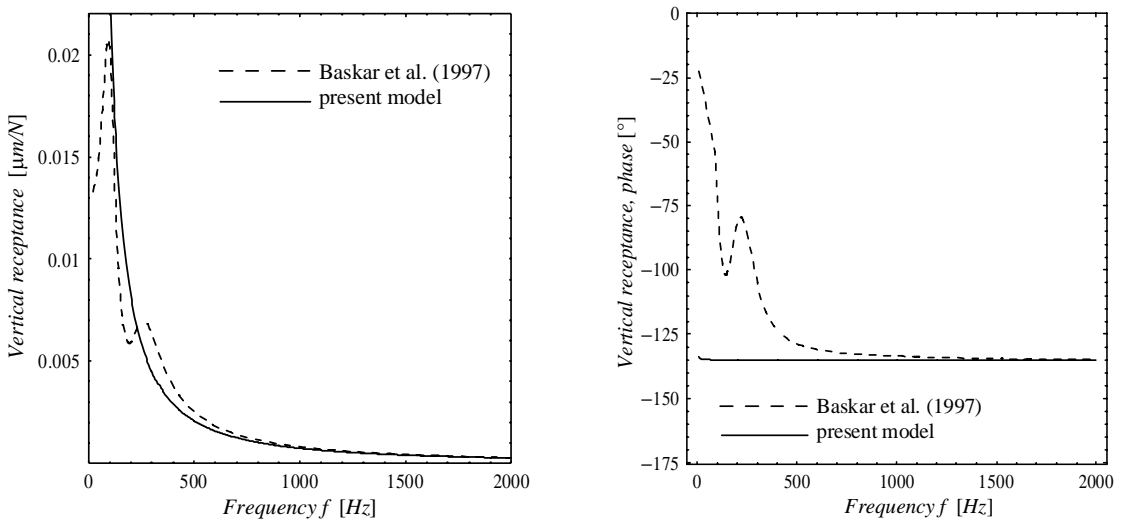

Figure 2. Vertical direct receptance ($E = 207$ GPa; $m_{\text{rail}} = 56$ kg/m; $m_w = 350$ kg; $V = 27.8$ m/s; $I_{\text{rail}} = 2.35 \times 10^{-5}$ m^4).
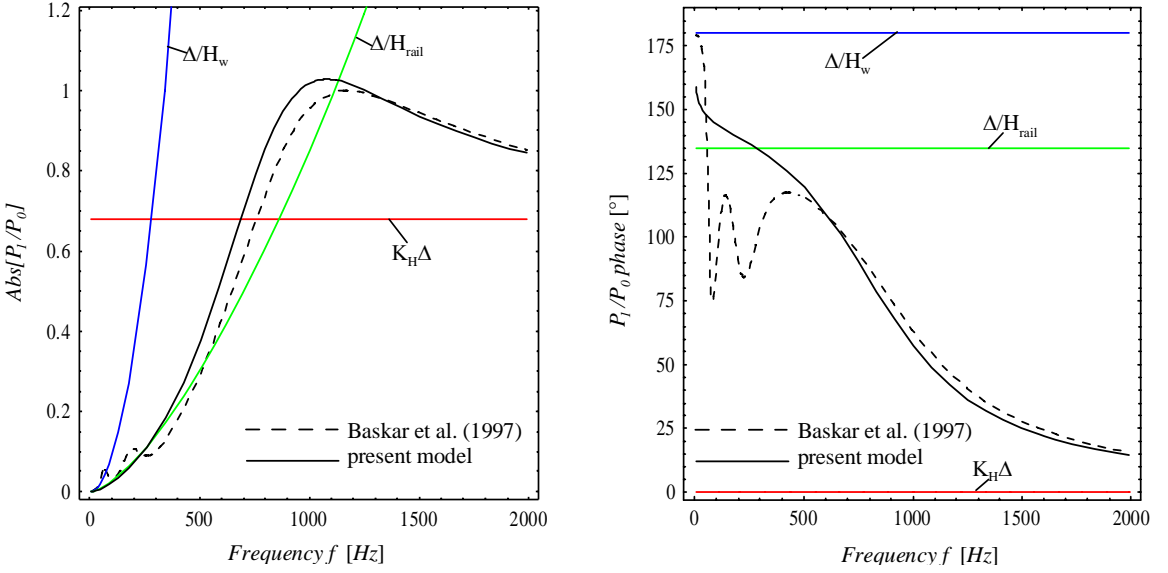
Figure 3. Normal load P_1/P_0 ($\Delta = 3.15 \times 10^{-5}$ m; $E = 207$ GPa; $m_{\text{rail}} = 56$ kg/m; $m_w = 350$ kg; $V = 27.8$ m/s; $I_{\text{rail}} = 2.35 \times 10^{-5}$ m^4).

Figure 3 shows the amplitude and phase of normal load P_1. The normal load is evaluated as

$$P_1 = \frac{\Delta}{H_{\text{rail}} + H_w + 1/k_H}, \tag{24}$$

where H_{rail}, H_w, $1/k_H$ are receptance of rail and wheel, respectively, and the inverse of Hertz stiffness. For H_w, we are simplifying the receptance with that of the concentrated mass,

$$H_w = -\frac{1}{m_w \omega^2} \tag{25}$$

and for the Hertz stiffness we use the expression

$$k_H = \left[\frac{6G^2 P_0 R_e}{(1 - \nu^2)} \right]^{1/3}. \tag{26}$$

To distinguish the various contributions, Figure 3 plots each term of the equation above Δ/H_{rail}, Δ/H_{wheel}, and $k_H \Delta$ separately, together with the resulting sum normalized with respect the mean normal load P_0 (the value of $\Delta = 3.15 \times 10^{-2}$ mm was taken such that the maximum value of P_1/P_0 is 1). The dominant effect at low f is the wheel, then the rail at intermediate frequencies. The phase moves from about 135° corresponding to the rail alone (somewhere near 300 Hz) down to 0° for the contact spring alone at very high frequencies.

4. Differential energy dissipation

We start with nominal conditions (normal load $P_0 = 50\ kN$, creepage -0.4%, BR rail geometry and wheels, mass of the wheel or wheelset 350 Kg, but inertia reduced using the formula $0.75 m_w R^2/2$).

Figure 4 shows contour plots of the real part of dissipation W_1 (ten equally spaced contours from 0 to the smallest value in the figure, which obviously is for the highest speed) with respect to the values of wavelength λ and speed V for tractive ratio $\tau = Q_0/\mu P_0 = 0.1$ and $\tau = 0.95$ (left and right panes, respectively) and for the simplified present model of the rail. Solid circles indicate the highest predicted growth for a given speed. In the plots the lines at constant frequency which gives the best fit of the minimum of real part of W_1 and experimental data points are also shown for reference. Notice for typical values of speed for which short pitch corrugation is observed ($\lambda = 20$–80 mm) the model gives the highest predicted growth at almost constant frequency, but a large area where growth is possible, and in good agreement with experimental data, except perhaps at the smallest speeds, where there seems to be some additional "filtering".

Figure 5 shows the same contour plots with the model of the rail in [Bhaskar et al. 1997a]. Similar results to Figure 4 are observed, especially at low tractive ratio (Figure 5, left). However, at low speeds, we have a new possible one or two other lines of possible growth at very low frequencies (about 180 Hz). This regime becomes more important at high tractive ratio (Figure 5, right), showing that the additional "filtering" is due to the low frequency receptance, deviating from the simpler Euler beam behaviour, i.e., due to the supports.

In Figure 6, left, we plot curves of the minima of dissipation (now in the dimensionless form $\hat{W}_1 = W_1/W_0$ which removes the linear dependence on speed) for different tractive ratio τ. The minima are evaluated by considering a window of variation for λ equal to 20–80 mm. It is clear that a constant value
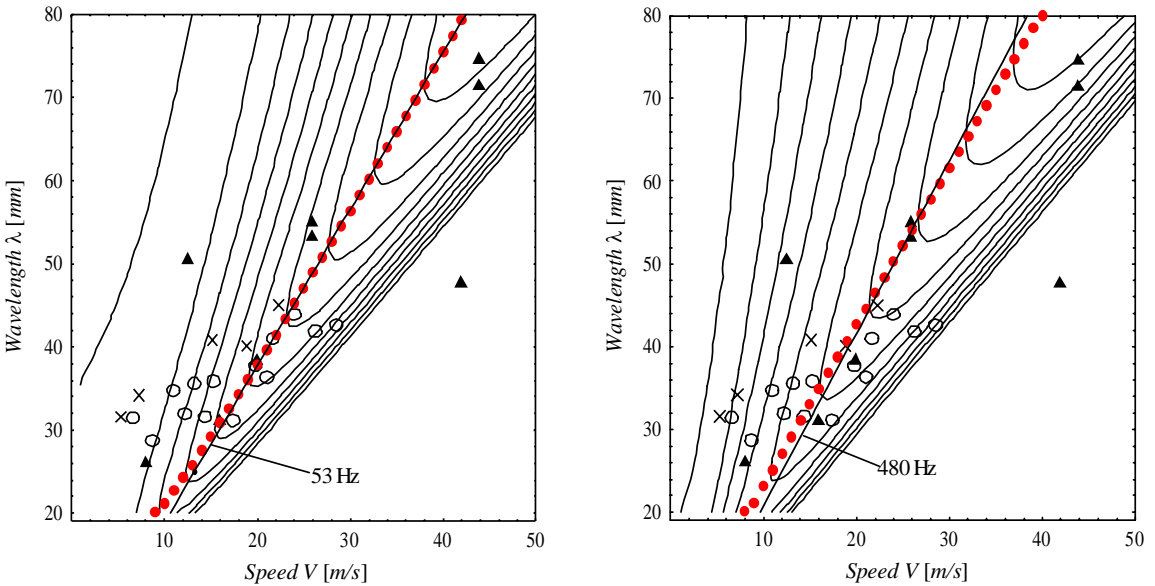

Figure 4. Contour plot of the real part of dissipation with respect to the initial undulation of the corrugation in term of λ and V, for calculations made using the present model (Euler beam for the rail): left, $\tau = 0.1$; right, $\tau = 0.95$. Solid circles indicate the highest predicted growth for a given speed. Data points from Figure 1 of [Bhaskar et al. 1997a] have been superimposed, as follows: open circles, BR survey (1911); triangles, Harrison (1979); crosses, Vancouver Skytrain (1992).
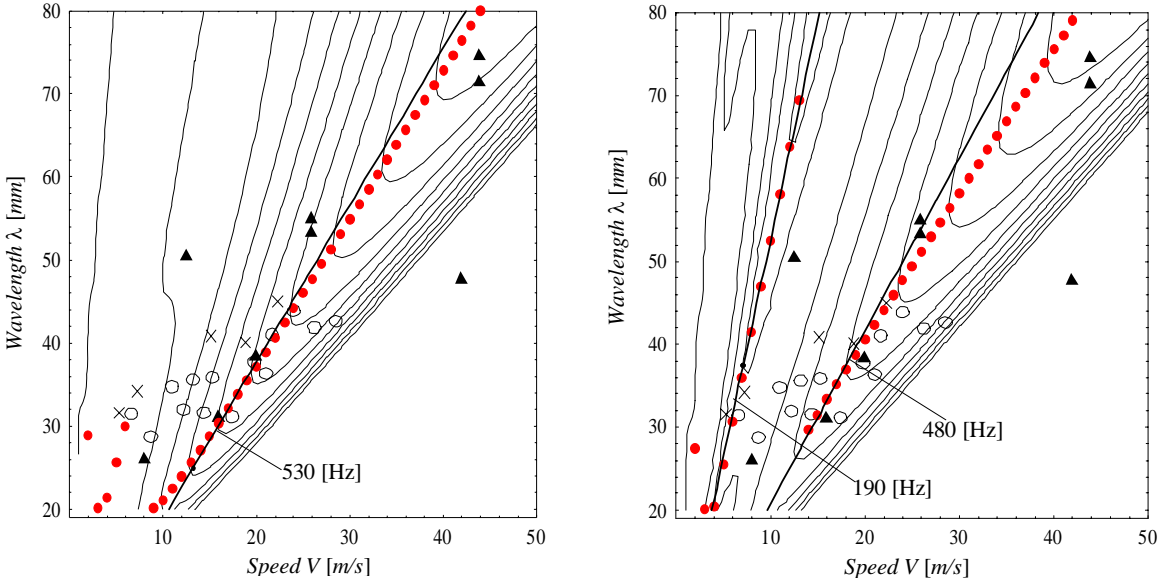
Figure 5. Counterpart of Figure 4 for calculations made using the model of [Bhaskar et al. 1997a]; see that figure for the legend.
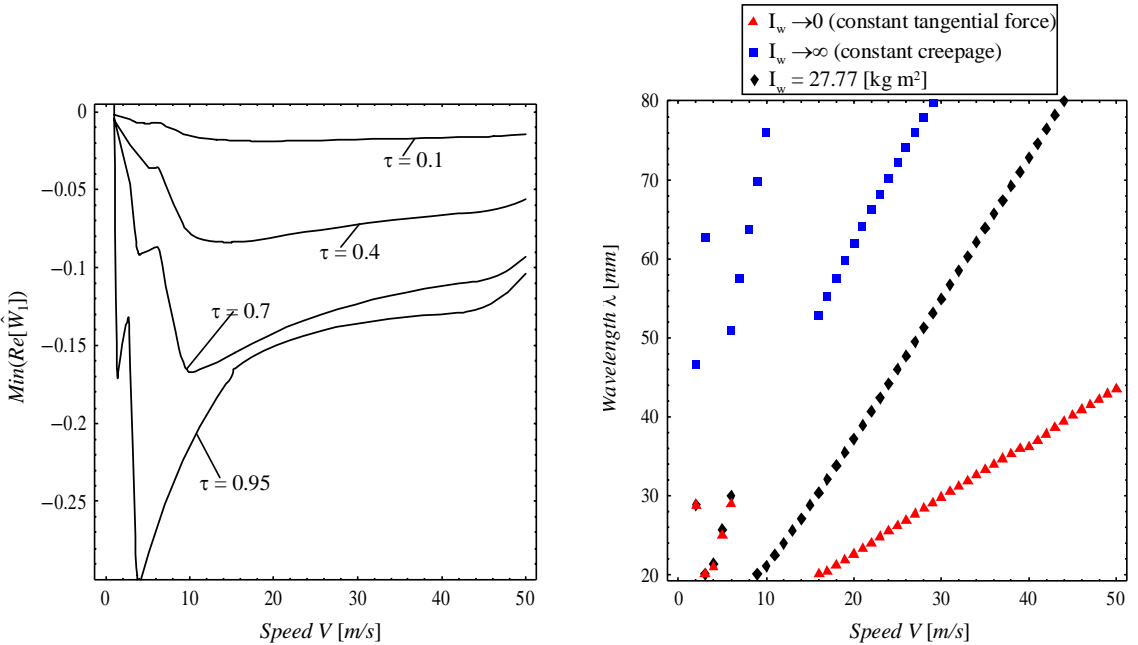

Figure 6. Left: Variation with the speed V of the maximum growth of dissipation, $\min(\hat{W}_1)$ for different tractive ratios. Right: Relation between the wavelength λ of corrugation and the speed V for which we have the maximum dissipation, for different values of inertia of the wheelset ($\tau = 0.1$). For both parts, $\Delta = 3.15 \times 10^{-5}$ m; $E = 207$ GPa; $\nu = 0.3$; $m_{\mathrm{rail}} = 56$ kg/m; $m_w = 350$ kg; $I_{\mathrm{rail}} = 2.35 \times 10^{-5}$ m^4; $\mu = 0.4$; $P_0 = 50$ kN; $R = 0.46$ m; $R_r = 0.23$ m.
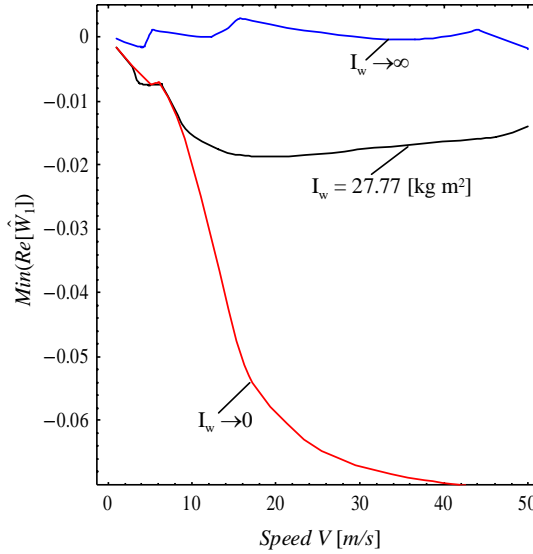
Figure 7. Variation with the speed V of the maximum growth of dissipation, $\min(\hat{W}_1)$, for different dissipation, for different values of inertia of the wheelset. ($\Delta = 3.15 \times 10^{-5}$ m; $E = 207$ GPa; $\nu = 0.3$; $m_{\text{rail}} = 56$ kg/m; $m_w = 350$ kg; $I_{\text{rail}} = 2.35 \times 10^{-5}$ m^4; $\mu = 0.4$; $\tau = 0.1$; $P_0 = 50$ kN; $R = 0.46$ m; $R_r = 0.23$ m.)

indicates here a linear increase with speed, and the deviations occurring mostly at high tractive ratio, are due to the switching from one frequency line to the other.

Figure 6, right, shows the relation between the wavelength λ of corrugation and speed V for which we have the maximum growth of dissipation for different inertia of the wheelset. In particular, the limit cases of constant tangential force ($I_w \to 0$) and constant creepage ($I_w \to \infty$) are plotted and compared with a typical case of inertia ($I_w = 27.77$ kg m^2). The limit cases can be considered as bounds for the values of (λ, V) which give growth of corrugation, and also explain why the assumptions of constant tangential load or constant creepage are significantly in error, particularly when considering also Figure 7 with the value of the dimensionless minima of $\hat{W}_1$ for the same cases of inertia considered in Figure 6. Again we can notice that constant tangential force and creepage bound the maximum growth of corrugation.

In Figure 8, for fixed speed ($V = 30$ m/s), we plot the variation of the minimum of $\hat{W}_1$ with the tractive ratio and inertia of wheelset, respectively. In the first case we have a monotonic decrease of the minimum of $\hat{W}_1$ (i.e. an increase of predicted exponential growth of corrugation) with τ. In the latter, an increase of the inertia I_w corresponds to a decrease of dissipation.

5. Discussion

Grassie and Johnson [1982a; 1982b; 1982c; 1982d] improved and extended beam models also to excitation on vertical, longitudinal and lateral excitation, using also careful experiments to compare the results. However, the wheelset dynamics has so many narrow resonances that its role is neglected. In the few cases where it is included, its role however seems crucial, perhaps even larger than what it really is, when considering other effects.
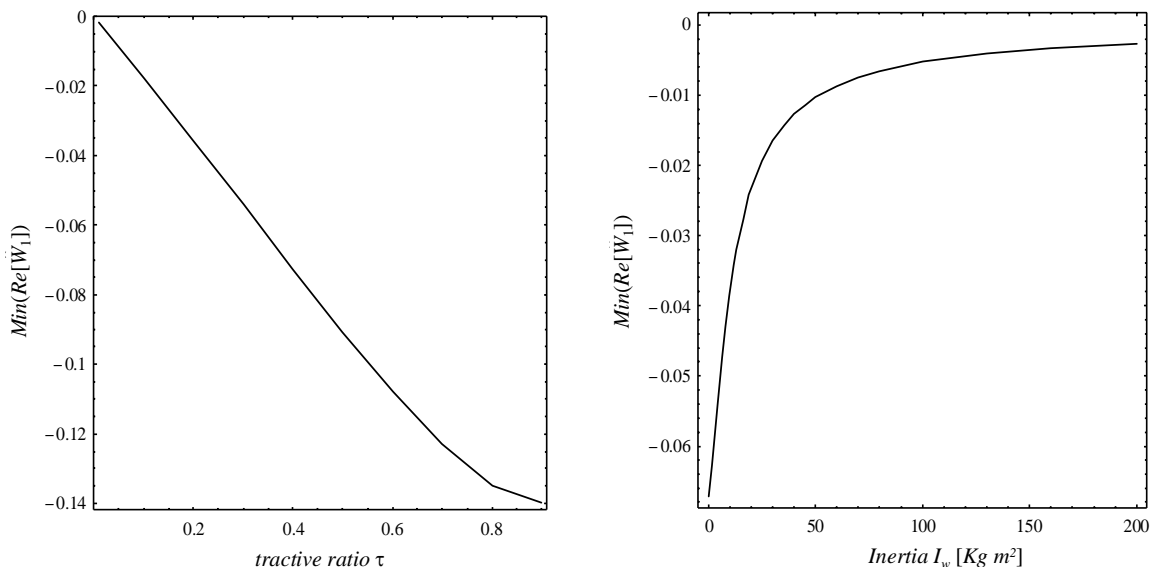
Figure 8. Variation with the tractive ratio τ (left) and with the inertia I_w (right) of the maximum growth of dissipation, $\min(\hat{W}_1)$, for fixed speed $V = 30$ m/s ($\Delta = 3.15 \times 10^{-5}$ m; $E = 207$ GPa; $\nu = 0.3$; $m_{\text{rail}} = 56$ kg/m; $m_w = 350$ kg; $I_{\text{rail}} = 2.35 \times 10^{-5}$ m^4; $\mu = 0.4$; $P_0 = 50$ kN; $R = 0.46$ m; $R_r = 0.23$ m; for the panel on the right, $\tau = 0.1$.)

For example:

(a) Tassilly and Vincents [1991a; 1991b] introduce the wheelset behaviour in full curve via its frequency response function, showing predominantly transversal wear on the leading wheelset corresponding to its first bending mode, and longitudinal wear on the rear one, related to the first torsional mode of the wheelset.

(b) Diana et al. [1998] suggest that the model of Tassilly and Vincents does not justify the case of changing corrugation with a simple change of the pad stiffness, as observed in the Milano subway they analyze. They notice corrugation wavelength is *not* driven by vertical resonances — neither the P2 frequency nor the pinned-pinned frequency (first bending mode) could correspond to the frequency of corrugation, and all the other higher resonant frequencies of the wheelset on the track do *not* change with the change from the stiff to the soft superstructure. Therefore they proposed a mechanism based on the discrete nature of the support and its periodic change of stiffness.

(c) Elkins et al. [1998], in a study of North American transit railways suggest the second torsional resonance of wheelset also at about 300 Hz as the fixing mechanism.

The closest to our model is in [Diana et al. 1998], the first part of which proposes a simple wheel with concentrated inertia and mass, rolling over a corrugated rail, in turn supported by a structure with periodic change of stiffness. The contact mechanics is simplified with a relationship similar to a Carter solution, although linear in normal load. However, their model is purely integrated in time, and results only for one specific case are illustrated, whereas here we explore fully the behaviour of the system by a perturbation

analysis, permitting to explore the growth of corrugation as a function of all the crucial various parameters. The model shows significant enhancement of corrugation growth with the periodic change of stiffness, which we shall include in later studies. This could be interpreted as inducing parametric resonance on the system, as studied by some authors more in the context of noise than corrugation (see, for example, [Wu and Thompson 2006; Sheng et al. 2006; Wu and Thompson 2004]). However, from these same studies, we expect that corrugation is enhanced in its growth and also modulated in amplitude, but not necessarily will change significantly its wavelength.

Hence, it seems surprising that the corrugation wavelengths may have been frequently associated to the pinned-pinned resonance at about 1000 Hz [Hempelmann and Knothe 1996; Müller 1999; 2000; 1998; Grassie 2005].[2]. Surprisingly, Hempelmann's thesis [1994], in Figure 7.15, has a full comparison of wavelength-speed like our Figure 1, two regimes are predicted around a 400 Hz line and around a 1450 Hz one, the first value not too far from one of our predictions. In [Hempelmann and Knothe 1996], reference to the 1450 Hz regime disappears, and instead there is a suggestion to the highest growth at the pinned-pinned resonance at 1060 Hz. Mueller, in his sophisticated nonlinear model [1999; 1998], seems to confirm Hempelmann's results, adding that other structural dynamics effects can also dominate the profile development, e.g. the high lateral rail receptance between 1600 and 1800 Hz and the low vertical rail receptance near 300 Hz. A detailed comparison is not possible but clearly would be interesting.

6. Conclusions

This note suggests a very simple model permitting a closed form treatment and full exploration of the phenomenon of corrugation with its possibly most crucial factors. The rotational dynamics of the wheel, which surprisingly is missing in many models, couples with the rotational dynamics with the vertical dynamics via the contact mechanics at the interface, leading to a strong effect of the train speed on the possible phase between normal load and local wear.

The results explain why Grassie and Johnson [1985] could not suggest an adequate mechanism, as the predicted phase corresponds to very large vehicle speeds, whereas our model shows that the phase between normal load and differential wear varies largely with speed, and hence should be included to justify the phenomenon.

The corrugation growth is found strongly increasing with the tractive ratio, and hence in stopping or departing conditions, the corrugation growth should be very high. This may explain the second observation of Grassie and Kalousek [1993], since a low normal load may increase the tractive ratio, and this may dominating over the decrease due to the fact that wear is also proportional to the dynamic normal load in turn proportional to the steady state mean value. A large inertia of the wheel may lower the speed for corrugation growth.

Appendix: Dynamic response of the rail

We consider the problem of an infinite beam subjected to a force that moves at speed V and whose magnitude oscillates in time at frequency $f = \omega/2\pi$ (where ω is the pulsation of the oscillation). In the

---

[2]Grassie reports that the pinned-pinned resonance is more precisely given as "about 800 Hz in the UK, for a sleeper spacing of 0.75 m and 56 kg/m rail, whereas in much of continental Europe it is more commonly about 1200 Hz because of the closer sleeper spacing (0.6 m) and heavier rail section (60 kg/m)."

steady state the vertical displacement of the beam will be of the form

$$u = U(x - Vt)\exp(\iota\omega t) \tag{27}$$

The equation on the motion for the beam, except under the load, is

$$\frac{dT}{dx} = -m\ddot{u},$$

where T is the shear force and m is the mass of the beam per unit length. From the linear elastic theory of the beam we also have

$$EI\frac{du^2}{dx^2} = M, \quad \frac{dM}{dx} = T,$$

where EI is the flexural rigidity of the beam and M is the bending moment. It follows that

$$EI\frac{d^4u}{dx^4} + m\frac{d^2u}{dt^2} = 0.$$

Now we introduce the damping in the above equation by adding the term $C\dot{u}$, giving

$$EI\frac{d^4u}{dx^4} + m\frac{d^2u}{dt^2} + C\frac{du}{dt} = 0, \tag{28}$$

where C is a damping coefficient.

By using (27) in (28) and cancelling the common factor $exp(\iota\omega t)$, we obtain

$$EIU^{IV} + m\left(V^2U'' - 2\iota V\omega U' - \omega^2 U\right) + C\left(-VU' + \iota\omega U\right) = 0.$$

If we introduce the following dimensionless variable ξ defined as

$$\frac{V\xi}{\omega} = x - Vt,$$

in which case

$$U'(x - Vt) = \frac{\omega}{V}U'(\xi)$$

etc., we obtain

$$KU^{IV}(\xi) + U''(\xi) - 2\iota U'(\xi) - U(\xi) + \hat{C}\left(-U'(\xi) + \iota U(\xi)\right) = 0,$$

where

$$K = \frac{EI\omega^2}{mV^4} = \frac{4\pi^2 EI}{mV^2\lambda^2} \tag{29}$$

is a dimensionless flexural rigidity and

$$\hat{C} = \frac{C}{m\omega} \ll 1.$$

Noting that the parameter $\lambda = 2\pi V/\omega$ is the wavelength of the implied corrugation.

The problem is therefore governed by the dimensionless parameters K and $\hat{C}$ and the phase shift between the excitation force and implied corrugation will be a function only of these parameters.

Solution. Equation (28) has the solution

$$U(\xi) = A \exp(s\xi),$$

where A is an arbitrary complex constant and s satisfies the fourth degree polynomial equation

$$Ks^4 + s^2 - 2\imath s - 1 + \hat{C}(-s + \imath) = 0$$

To avoid the complex coefficient in this equation, we can write

$$s = \imath\sigma,$$

giving

$$K\sigma^4 - \sigma^2 + 2\sigma - 1 + \hat{C}(-\imath\sigma + \imath) = 0. \tag{30}$$

For $\hat{C} = 0$ the solutions of (30) are

$$\sigma_{1,2} = \frac{1 \pm \sqrt{1 - 4k}}{2k}; \qquad \sigma_{3,4} = \frac{-1 \pm \sqrt{1 + 4k}}{2k},$$

where $k^2 = K$.

We notice that all the roots are real if $k < 1/4$ and hence $K < 1/16$. For $K > 1/16$, $\sigma_{1,2}$ are complex and $\sigma_{3,4}$ are real. This in turn implies that roots for s are either all pure imaginary, or else two are complex and two are imaginary. The imaginary roots correspond to waves of constant amplitude, so it is difficult to know what to do about conditions at infinity. Physically, this corresponds to the fact that the undamped beam can support free vibrations and if the wavelength of these are suitably chosen, they can be combined to give a travelling wave of any given speed. We can get around it by imposing a small amount of damping.

Our concern is with the two real roots $\sigma_{3,4}$ and we anticipate that for small $\hat{C}$ we can modify them in the form

$$\sigma_3 = \frac{-1 + \sqrt{1 + 4k}}{2k} + \hat{C}g_3(k); \qquad \sigma_4 = \frac{-1 - \sqrt{1 + 4k}}{2k} + \hat{C}g_4(k).$$

Differentiating (30) with respect to $\hat{C}$, we have

$$\left(4K\sigma^3 - 2\sigma + 2 - \hat{C}\imath\right)\frac{d\sigma}{d\hat{C}} - \imath(\sigma - 1) = 0,$$

and hence

$$\frac{d\sigma}{d\hat{C}} = \frac{\imath(\sigma - 1)}{4K\sigma^3 - 2\sigma + 2 - \hat{C}\imath}.$$

Substituting $\sigma = \sigma_3$ and $\hat{C} = 0$, we obtain:

$$g_3(k) = \frac{d\sigma}{d\hat{C}} = -\frac{\imath}{2\sqrt{1 + 4k}}.$$

which shows that $\imath g_3(k)$ is always positive, hence the real part of the modified root s_3 is positive.

Next substitute $\sigma = \sigma_4$ so that

$$g_4(k) = \frac{d\sigma}{d\hat{C}} = \frac{\imath}{2\sqrt{1 + 4k}}.$$

Apart from the ι factor, this is positive for all k and hence $\iota g_4(k) < 0$ and the real part of the modified root s_4 is negative.

Boundary conditions. We construct a solution for the region $\xi > 0$ using the roots with negative real part, so

$$U(\xi) = A_1 \exp(s_1\xi) + A_4 \exp(s_4\xi).$$

For $\xi < 0$, we use the roots with positive real part giving

$$U(\xi) = A_2 \exp(s_2\xi) + A_3 \exp(s_3\xi).$$

We require continuity in u and its first two derivatives (the second derivatives to achieve continuity of bending moment M), giving

$$A_1 + A_4 = A_2 + A_3, \qquad A_1 s_1 + A_4 s_4 = A_2 s_2 + A_3 s_3, \qquad A_1 s_1^2 + A_4 s_4^2 = A_2 s_2^2 + A_3 s_3^2. \qquad (31)$$

The final equation comes from the requirement that the shear force has a discontinuity of magnitude $F_0 \exp(\iota\omega t)$ at the origin. In other words

$$T(0^+) - T(0^-) = F_0 \exp(\iota\omega t),$$

which implies

$$\frac{EI\omega^3}{V^3}\left(U'''(0^+) - U'''(0^-)\right) = F_0. \qquad (32)$$

We therefore have

$$A_1 s_1^3 + A_4 s_4^3 - A_2 s_2^3 - A_3 s_3^3 = \frac{F_0 V^3}{EI\omega^3}.$$

The receptance will be determined by the complex ratio between F_0 and the displacement under the load which is

$$u_0 = A_1 + A_4. \qquad (33)$$

It will be a function of K (and hence of the frequency f). Notice that this is physically meaningful only above the value of K that makes $g_3(K) > 0$. Further the result will be only slightly affected by g_3 and g_4 as long as these are small, and hence we can simplify the problem by setting these to zero.

Large K limit. Consider the case where $K \gg 1$, which is equivalent to $V \to 0$ in view of (29). In other words, in this limit, we should recover the solution for an oscillating load that is stationary at the origin. The roots then tend to the values

$$s_1 = -\frac{1}{\sqrt{k}}; \qquad s_2 = \frac{1}{\sqrt{k}}; \qquad s_3 = \frac{\iota}{\sqrt{k}}; \qquad s_4 = -\frac{\iota}{\sqrt{k}},$$

and from the boundary conditions (31), (32) and (33), we then get

$$u_0 = -\frac{F_0(1+\iota)}{4(m^3 EI)^{1/4}\omega^{3/2}}.$$

Thus,

$$u(0) = u_0 \exp(\iota\omega t) = -\frac{F_0(1+\iota)}{4(m^3 EI)^{1/4}\omega^{3/2}}\exp(\iota\omega t),$$

which we can rewrite as

$$u\left(0\right) = \frac{F_0}{2\sqrt{2}\left(m^3 E I\right)^{1/4} \omega^{3/2}} \exp\left(\iota\left(\omega t - 3\pi/4\right)\right).$$

Thus, the displacement lags from the force by $3\pi/4 = 135°$.

The vertical receptance can hence be written as

$$H_{\text{rail}} = \frac{u\left(0\right)}{F_0} = \frac{\exp\left(-\iota 3\pi/4\right)}{2\sqrt{2}\left(m^3 E I\right)^{1/4} \omega^{3/2}}.$$

References

[Bhaskar et al. 1997a] A. Bhaskar, K. L. Johnson, G. D. Wood, and J. Woodhouse, "Wheel-rail dynamics with closely conformal contact, 1: Dynamic modelling and stability analysis", *Proc. Inst. Mech. Eng. F, J. Rail Rapid Transit* **211**:1 (1997), 11–26.

[Bhaskar et al. 1997b] A. Bhaskar, K. L. Johnson, and J. Woodhouse, "Wheel-rail dynamics with closely conformal contact, 2: Forced response, results and conclusions", *Proc. Inst. Mech. Eng. F, J. Rail Rapid Transit* **211**:1 (1997), 27–40.

[Both et al. 2001] J. A. Both, D. C. Hong, and D. A. Kurtze, "Corrugation of roads", *Physica A* **301**:1–4 (2001), 545–559.

[Carson and Johnson 1971] R. M. Carson and K. L. Johnson, "Surface corrugations spontaneously generated in a rolling contact disc machine", *Wear* **17**:1 (1971), 59–72.

[Diana et al. 1998] G. Diana, F. Cheli, S. Bruni, and A. Collina, "Experimental and numerical investigation on subway short pitch corrugation", *Veh. Syst. Dyn.* **29**:S1 (1998), 234–245.

[Elkins et al. 1998] J. A. Elkins, S. Grassie, and S. Handal, "Rail corrugation mitigation in transit", *TCRP Resarch Results Digest* **26** (1998), 1–33.

[Frederick 1987] C. O. Frederick, "A rail corrugation theory", pp. 181–211 in *Contact mechanics and wear of rail/wheel systems, II: Proceedings of the International Symposium* (Kingston, RI, 1986), edited by G. M. L. Gladwell et al., University of Waterloo Press, Waterloo, ON, 1987.

[Grassie 2005] S. L. Grassie, "Rail corrugation: advances in measurement, understanding and treatment", *Wear* **258**:7-8 (2005), 1224–1234.

[Grassie and Edwards 2008] S. L. Grassie and J. W. Edwards, "Development of corrugation as a result of varying normal load", *Wear* **265**:9–10 (2008), 1150–1155.

[Grassie and Johnson 1985] S. L. Grassie and K. L. Johnson, "Periodic microslip between a rolling wheel and a corrugated rail", *Wear* **101**:4 (1985), 291–309.

[Grassie and Kalousek 1993] S. L. Grassie and J. Kalousek, "Rail corrugation: characteristics, causes and treatments", *Proc. Inst. Mech. Eng. F, J. Rail Rapid Transit* **207**:1 (1993), 57–68.

[Grassie et al. 1982a] S. L. Grassie, R. W. Gregory, D. Harrison, and K. L. Johnson, "The dynamic response of railway track to high frequency vertical excitation", *J. Mech. Eng. Sci.* **24**:2 (1982), 77–90.

[Grassie et al. 1982b] S. L. Grassie, R. W. Gregory, and K. L. Johnson, "The dynamic response of railway track to high frequency lateral excitation", *J. Mech. Eng. Sci.* **24**:2 (1982), 91–96.

[Grassie et al. 1982c] S. L. Grassie, R. W. Gregory, and K. L. Johnson, "The dynamic response of railway track to high frequency longitudinal excitation", *J. Mech. Eng. Sci.* **24**:2 (1982), 97–102.

[Grassie et al. 1982d] S. L. Grassie, R. W. Gregory, and K. L. Johnson, "The behaviour of railway wheelsets and track at high frequencies of excitation", *J. Mech. Eng. Sci.* **24**:2 (1982), 103–111.

[Groß-Thebing 1993] A. Groß-Thebing, *Lineare Modellierung des instationären Rollkontaktes von Rad und Schiene*, Fortschritt-Berichte VDI, 12: Verkehrstechnik/Fahrzeugtechnik **199**, VDI, Düsseldorf, 1993.

[Hempelmann 1994] K. Hempelmann, *Short pitch corrugation on railway rails: a linear model for prediction*, Fortschritt-Berichte VDI, 12: Verkehrstechnik/Fahrzeugtechnik **231**, VDI, Düsseldorf, 1994.

[Hempelmann and Knothe 1996] K. Hempelmann and K. Knothe, "An extended linear model for the prediction of short pitch corrugation", *Wear* **191**:1–2 (1996), 161–169.

[Hoffmann and Misol 2007] N. P. Hoffmann and M. Misol, "On the role of varying normal load and of randomly distributed relative velocities in the wavelength selection process of wear-pattern generation", *Int. J. Solids Struct.* **44**:25-26 (2007), 8718–8734.

[Johnson and Gray 1975] K. L. Johnson and G. G. Gray, "Development of corrugations on surfaces in rolling contact", *Proc. Inst. Mech. Eng.* **189** (1975), 567–580.

[Müller 1998] S. Müller, *Linearized wheel-rail dynamics: stability and corrugation*, Fortschritt-Berichte VDI, 12: Verkehrstechnik/Fahrzeugtechnik **369**, VDI, Düsseldorf, 1998.

[Müller 1999] S. Müller, "A linear wheel-track model to predict instability and short pitch corrugation", *J. Sound Vib.* **227**:5 (1999), 899–913.

[Müller 2000] S. Müller, "A linear wheel-rail model to investigate stability and corrugation on straight track", *Wear* **243**:1–2 (2000), 122–132.

[Sato et al. 2002] Y. Sato, A. Matsumoto, and K. Knothe, "Review on rail corrugation studies", *Wear* **253**:1–2 (2002), 130–139.

[Sheng et al. 2006] X. Sheng, D. J. Thompson, C. J. C. Jones, G. Xie, S. D. Iwnicki, P. Allen, and S. S. Hsu, "Simulations of roughness initiation and growth on railway rails", *J. Sound Vib.* **293**:3-5 (2006), 819–829.

[Tassilly and Vincent 1991a] E. Tassilly and N. Vincent, "A linear model for the corrugation of rails", *J. Sound Vib.* **150**:1 (1991), 25–45.

[Tassilly and Vincent 1991b] E. Tassilly and N. Vincent, "Rail corrugations: analytical model and field tests", *Wear* **144**:1-2 (1991), 163–178.

[Valdivia 1988a] A. Valdivia, *Die Wechselwirkung zwischen hochfrequenter Rad-Schiene-Dynamik und ungleichförmigem Schienenverschleiss: ein lineares Modell*, Fortschritt-Berichte VDI, 12: Verkehrstechnik/Fahrzeugtechnik **93**, VDI, Düsseldorf, 1988.

[Valdivia 1988b] A. Valdivia, "A linear dynamic wear model to explain the initiating mechanism of corrugation", pp. 493–496 in *The dynamics of vehicles on roads and on tracks: Proceedings of 10th IAVSD Symposium* (Prague, 1987), edited by M. Apetaur, Swets & Zeitlinger, Amsterdam, 1988.

[Wu and Thompson 2004] T. X. Wu and D. J. Thompson, "On the parametric excitation of the wheel/track system", *J. Sound Vib.* **278**:4-5 (2004), 725–747.

[Wu and Thompson 2006] T. X. Wu and D. J. Thompson, "On the rolling noise generation due to wheel/track parametric excitation", *J. Sound Vib.* **293**:3-5 (2006), 566–574.

LUCIANO AFFERRANTE: luciano@poliba.it
CEMEC-PoliBA, Via le Japigia 182, Politecnico di Bari, 70125 Bari, Italy

MICHELE CIAVARELLA: mciava@poliba.it
CEMEC-PoliBA, Via le Japigia 182, Politecnico di Bari, 70125 Bari, Italy